Magnetic and transport properties of $Yb_{1-x}Gd_xTe$

D. Ravot
Laboratoire de Chimie Métallurgique des Terres Rares, Centre National de la Recherche Scientifique, 1 place A. Briand, 92190 Meudon, France

A. Mauger
Groupe de Physique des Solides, Universités Paris 7 et Paris 6, 2 place Jussieu, 75251 Paris Cedex 05, France

O. Gorochov
Laboratoire de Physique des Solides, Centre National de la Recherche Scientifique, 1 place A. Briand, 92190 Meudon, France

(Received 7 April 1993; revised manuscript received 28 June 1993)

Both magnetic and transport properties of $Yb_{1-x}Gd_xTe$ solid solutions have been investigated in the whole range $0<x<1$, for temperatures $4.2<T<300$ K. Antiferromagnetic ordering is observed above the magnetic percolation threshold $x_c \approx 0.45$, due to the indirect exchange interaction between the localized magnetic moments carried by Gd^{3+} ions, mediated via the free carriers. The Gd^{3+} ions also act as donors, hence a metal-insulator transition at $x_m \approx 0.2$. This concentration is one order of magnitude larger than predicted by the Mott criterion, due to the important role played by magnetic fluctuations in the localization process. Pretransitional effects are investigated in the metallic side, within the framework of existing theories on disordered metals. A model taking into account the electron scattering by phonons, localized spin fluctuations, and Coulomb interactions allows for an overall agreement between the theoretical and experimental resistivity curves, at any x. In particular, a T-linear dependence of the conductivity is observed in the strong diffusion regime $x_m<x<0.5$, in a range of temperature that extends up to 50 K. We attribute this behavior to the electron-electron scattering that dominates the transport properties in a material which proves to be a unique example of disordered metals with a high electron density (due to the high value of x_c).

I. INTRODUCTION

The solid solution $Yb_{1-x}Gd_xTe$ crystallizes in the fcc structure in the whole range of composition $0 \le x \le 1$.[1] Since the ytterbium is divalent, YbTe is a nonmagnetic semiconductor. The Gd^{3+} ions carry a spin $S=\frac{7}{2}$, and thus introduce a magnetism of localized moments. In particular, GdTe is a II-type antiferromagnet.[2] Gd^{3+} ions also play the role of donor, so that a metal-insulator transition (MIT) will occur at some finite concentration x_m of dopant. In nonmagnetic materials, this transition has been extensively studied in the past, both theoretically and experimentally.[3] The MIT in $Yb_{1-x}Gd_xTe$, however, is different because it is greatly influenced by the exchange interaction $J_{df}S\cdot s$ between the donor electron in excess in a d orbital and the localized spin of the $4f^7$ shell. In the semiconductor side of the MIT, for example, the electron bound to a donor can spin polarize the localized moment in its vicinity to gain a magnetic exchange contribution to the binding energy and form the so-called bound magnetic polaron (BMP). This increase of binding energy also means a shrinking of the electron orbital, which has been extensively studied in other magnetic semiconductors.[4] It follows that the magnetic interaction contributes significantly to the electron localization. An evidence of this effect is the very large value of x_m, which we find equal to 0.28, one order of magnitude larger than predicted by the Mott criterion. In the metallic side of the MIT, all the donors are ionized, so large x_m also means a large concentration n of conduction electrons even close to x_m. This material thus provides a unique opportunity to explore the properties of disordered metals with high electron densities, in the strong diffusion regime.

The main purpose of this paper is the study of the metal-insulator transition in $Yb_{1-x}Gd_xTe$, with emphasis on the properties of the disordered metal, through analysis of the resistivity curves. The importance of the exchange interaction between the donor electrons and the magnetic subsystem implies a strong correlation between the magnetic and transport properties, which must then be investigated simultaneously. Details of the synthesis of homogeneous samples with final compositions close to the initial one, and of crystallizing in a single phase, have been reported elsewhere.[1] Both magnetic susceptibility and resistivity curves have been measured in the temperature range $4.2 \le T \le 300$ K for samples of various compositions exploring the whole range $0 \le x \le 1$. The magnetic phase diagram illustrates that the magnetic percolation threshold for the onset of long-range magnetic ordering is $x_c \cong 0.4$. We argue that the Ruderman-Kittel-Kasuya-Yoshida (RKKY) indirect exchange interaction[5] mediated by the free carriers is responsible for the magnetic ordering above x_c. This is consistent with the fact that

$x_m < x_c$, i.e., long-range antiferromagnetic ordering is observed only in metallic samples. This is also consistent with our claim that the exchange interaction $J_{df}S\cdot s$ is of primary importance, since the RKKY interaction is just proportional to $(J_{df})^2$. The exchange interaction between the free carriers and the localized spins is also responsible for a critical scattering of the free carriers by the fluctuations of the localized spins in the vicinity of the Néel temperature, also studied in this work. There is a whole range $x_m < x < x_c$, however, where there is no antiferromagnetic ordering, so that the diffusion of the free carriers by spin fluctuation does not contribute significantly to the temperature dependence of the resistivity curves. The outstanding temperature dependence of the resistivity in this case is then analyzed within the framework of existing theories on disordered metals. The data suggest that electron-electron Coulomb interactions are very important because of the high electron density, and are responsible for the diffusion of the conduction electrons at low temperature in this range of gadolinium concentrations. The paper is organized as follows: the magnetic properties are reported in Sec. II. The transport properties are the subject of Sec. III. Section IV is devoted to a discussion of the results.

II. MAGNETIC PROPERTIES

The magnetic susceptibility curves $\chi(T)$ have been measured for all samples and some of them are illustrated in Fig. 1. For $x \geq 0.5$, $\chi(T)$ goes through a maximum, which can be attributed to the antiferromagnetic ordering at the Néel temperature T_N. As x decreases, the peak in $\chi(T)$ is smoothed, and for $x < 0.5$, no maximum can be observed in the $\chi(T)$ curve. Instead, a plateau is observed below a temperature we call T_f. This plateau extends down to the lowest temperature investigated. The different nature of the spin freezing on both sides of $x = 0.5$ is also evidenced in the different x dependences of T_N and T_f illustrated in Fig. 2. While T_N is an increasing function of x, T_f is almost independent of x. This feature is proof that T_f is not related to a collective freezing in the spin system. It is, rather, associated with the local freezing of magnetic clusters of finite size, which exist in finite numbers even if the magnetic ions are randomly distributed in the material. The magnetic percolation threshold can be estimated by extrapolation of the $T_N(x)$ curve to $T_N = 0$ (see Fig. 2): $x_c = 0.45 \pm 0.04$.

The Curie-Weiss law $\chi^{-1}(T)\alpha(T - \Theta_p)$ is well satisfied above 150 K for any x. This is illustrated in Fig. 3 for $x = 0.5$. Note, however, that a reliable determination of the paramagnetic Curie temperature requires an extension of data up to temperatures many times Θ_p, say at least 600 K in the occurrence. Therefore, it is not clear to what extent the parameter Θ_p determined from the $\chi^{-1}(T)$ data in the small temperature range 150–300 K available in the experiments is a good estimate of the paramagnetic Curie temperature. Nevertheless, analysis of the variations of Θ_p with x proved useful in demonstrating that the RKKY interaction is dominant for $x \geq 0.4$,[1] while another mechanism is responsible for the magnetic interaction in the comparison range $x \leq 0.2$, which is, to our knowledge, the first evidence that this is the range of composition where the material is in the insulating phase.[1]

In the metallic configuration, the RKKY interaction between two localized spins S_i and S_j separated by the distance R_{ij} can be written as

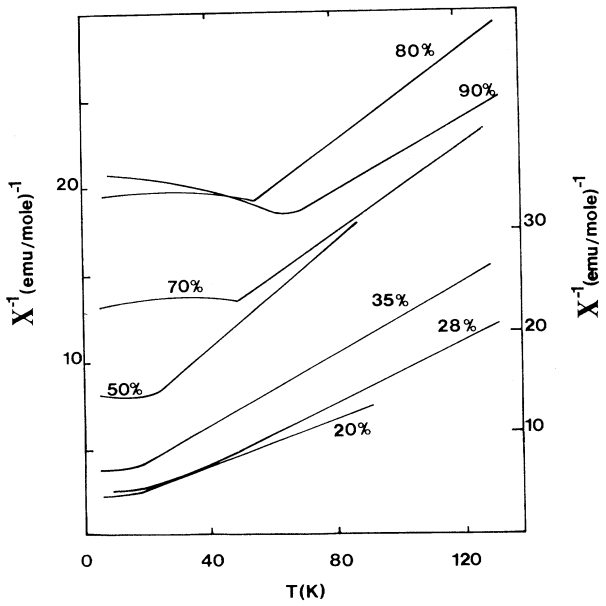

FIG. 1. Inverse of the magnetic susceptibility as a function of temperature for various gadolinium concentrations $x > 0.4$ (left scale) and $x < 0.4$ (right scale). Note the extremum of the curves for $x > 0.4$, at a temperature we identify as the Néel temperature. At low Gd concentrations, only a broad plateau is observed below a spin-freezing temperature T_f.

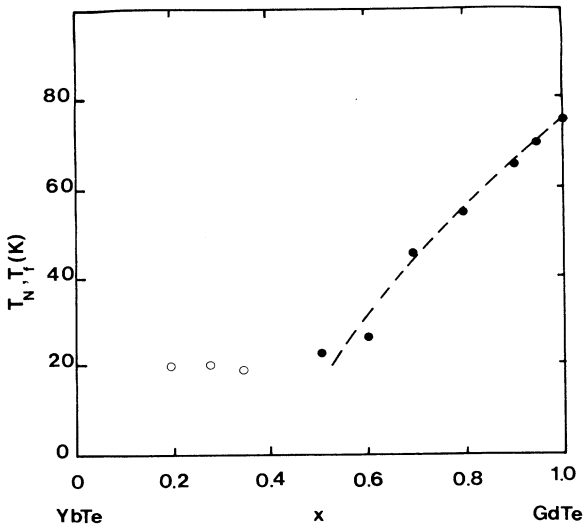

FIG. 2. Néel temperature (●) and spin-freezing temperature T_f(○) as functions of the gadolinium concentration x. The broken curve is a guide for the eyes.

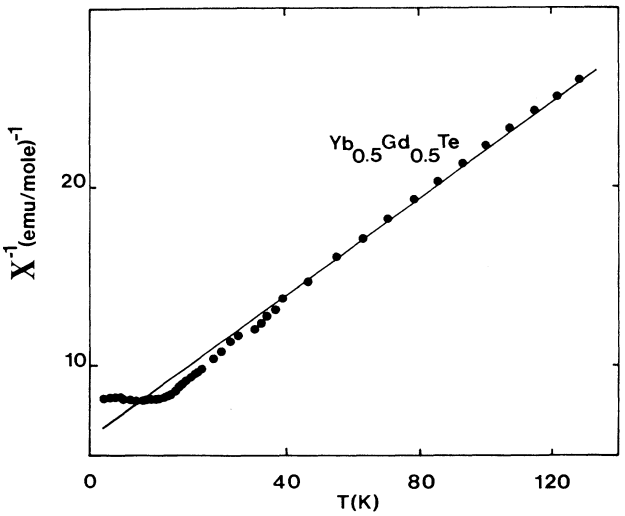

FIG. 3. Inverse of the magnetic susceptibility as a function of temperature of the $x=0.5$ sample. The dots are experimental data, the straight line has been drawn to illustrate the deviations from the Curie-Weiss law for $T<40$ K.

$$H=-\sum_{i,j} J(R_{ij})\mathbf{S}_i\cdot\mathbf{S}_j \ ,$$
$$J(R_{ij})=\frac{n^2}{E_F}J_{df}^2\frac{\sin(2k_FR_{ij})-2k_FR_{ij}\cos(2k_FR_{ij})}{(2k_FR_{ij})^4} \times e^{-R_{ij}/\lambda} \ , \quad (1)$$

where n is the concentration of the conduction electrons and k_F is the wave vector at the Fermi energy E_F. The exponential factor is the correlation introduced by de Gennes[6] to account for the fact that the mean free path λ of the electron is finite, and plays the role of a cutoff for the RKKY interaction. Transport properties will show that λ is small, so the magnetic properties of the localized moments are dominated by the exchange coupling at short distance, i.e., $J(R)$ where R is the mean distance between magnetic ions. In particular, the antiferromagnetism encountered in this material implies that R is larger than the extension $\cong k_{F^{-1}}$ of the ferromagnetic cloud. Also, we note that in the metallic configuration where each gadolinium contributes one electron in the conduction band, $k_F \alpha x^{1/3}$, while $R \alpha x^{-1/3}$, so that k_FR is independent of x. Note, however, that the approximation $R \alpha x^{-1/3}$ is valid for some range, but is likely to be too crude for high concentrations, where it is more reasonable to look at the probability of occupation of neighbor sites at fixed distances. This fact restores a dependence of k_FR on x which, however, remains small, so that the exchange constant $J(R)$ does not change sign with x in Eq. (1). This is, in essence, the reason why the long-range order is always the same, namely, antiferromagnetic for any x in the range $x>x_c$.

Deviations from the Curie-Weiss law can be observed for $T<150$ K in the susceptibility curves of samples with $x\leq 0.5$. The breakdown of the mean-field approximation (MFA) and, thus, of the Curie-Weiss law, is expected to occur at low temperatures, due to the increasing importance of spin-correlation effects. In antiferromagnetic compounds, where the magnetic ions are not dilute, such deviations are observed only close to T_N, and yet they correspond to experimental values of the magnetic susceptibility smaller than those predicted by the Curie-Weiss law. Just the opposite is observed in the present case (Fig. 3). For these reasons, the increase of $\chi(T)$ and $|\Theta_p|$ in the range $x_m\leq x\leq 0.5$ with respect to the MFA is of a different nature, and can be regarded as characteristic of disordered metals in the region close to the MIT, where electron and spin density fluctuations are important. Indeed, such an increase of χ is predicted by the theories of disordered metals.[7] Transport experiments in the next section will confirm that this range of composition $x_m\leq x\leq 0.5$ is the domain where the physical properties are dominated by the MIT pretransitional effects.

III. TRANSPORT PROPERTIES

Hall-effect measurements reveal that the carrier concentration is essentially independent of the temperature in the range $77<T<300$ K for $x\geq 0.28$. Moreover, it is found to be in quantitative agreement with the value predicted on the basis that each Gd ion contributes one electron in the conduction band, within a few percent. For $x\geq 0.28$, the samples have thus a metallic character.

Resistivity curves have been investigated for temperatures in the range $4.2<T<300$ K. The results are illustrated in Figs. 4–6 for various compositions. Qualitative differences are observed in the shape of the $\rho(T)$ curves, on both sides of the magnetic percolation threshold.

For $x\geq 0.5$, the scattering of the free carriers by spin fluctuations is important at low temperatures where the

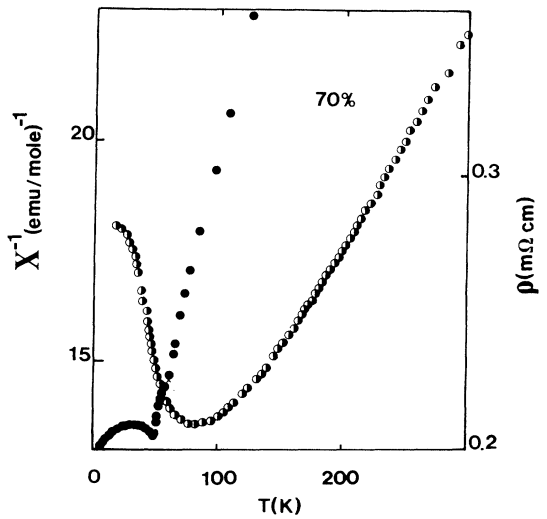

FIG. 4. Resistivity curve (■) of $Yb_{1-x}Gd_xTe$, for a typical gadolinium concentration above the magnetic percolation threshold: $x=0.7$. Note the sharp increase of the resistivity upon cooling at low temperature; the inflection point of the resistivity curve corresponding to the Néel temperature defined by the peak of the magnetic susceptibility curve (●) is also reported for comparison.

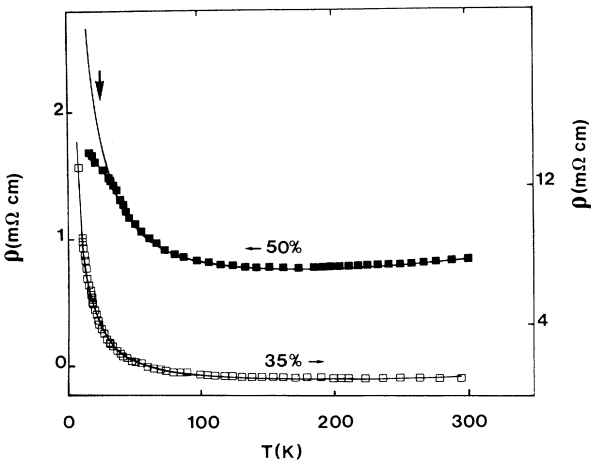

FIG. 5. Resistivity curves for two samples with gadolinium concentrations $x=50\%$ (left scale) and 35% (right scale). The full lines are theoretical curves in a model that neglects the temperature dependence of the scattering of the free carriers by spin fluctuations (see text); hence the deviation between theory and experiment for the sample with $x=50\%$ in the antiferromagnetic configuration. The Néel temperature T_N for $x=50\%$ is marked by an arrow. Quantitative agreement between theory and experiments is achieved down to the lowest temperature investigated for $x=35\%$, which is smaller than the magnetic percolation threshold (see Fig. 2).

phonon effects become negligible. This is best evidenced by the sharp variations of ρ in the vicinity of T_N illustrated, for example, in Fig. 4 for $x=0.7$. On the other hand, at temperatures $T \gg T_N$ where magnetic correlations are negligible, the scattering of the free carriers by phonons dominates and is responsible for an increase of ρ with T. The importance of phonon effects decreases as a function of x. This is evidenced by the decrease of the slope of $\rho(T)$ as x decreases from 0.7 to 0.5, in the range $T \geq 200$ K, where the increase of ρ with T is quasilinear.

For $x<0.5$, ρ weakly increases at high temperature

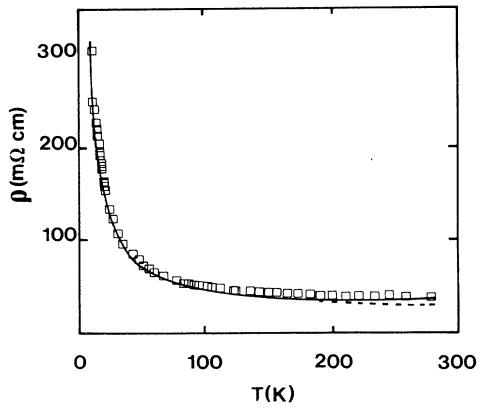

FIG. 6. Resistivity curve of $Yb_{1-x}Gd_xTe$ for $x=28\%$. The full (broken) curves are theoretical fits in a model of disordered metals, which includes (does not include) the scattering of the electrons by phonons.

only. Therefore, the dominant mechanism of diffusion for the free carriers is no longer related to the phonons. It will be shown in Sec. IV that this behavior of the resistivity is attributable to quantum corrections, and is a pretransitional effect when the metal-insulator transition in these disordered magnetic materials is approached from the metallic side for $x \geq 0.28$. An activated regime is observed at still lower gadolinium concentrations, where the weak localization regime is reached. Let us now detail the analysis of the transport properties, depending on the concentration x of magnetic ions.

A. Case $x>0.5$

According to the previous discussion, the resistivity can be written in the form

$$\rho=\rho_0+\rho_{\rm ph}+\rho_m \ , \tag{2}$$

with ρ_0 the residual resistivity of the metallic samples; $\rho_{\rm ph}$ and ρ_m are the contributions to ρ associated with the scattering of the free carriers by phonons and magnetic fluctuations, respectively. $\rho_{\rm ph}$ can be modelized within the framework of the Grüniesen-Bloch model, according to which

$$\rho_{\rm ph}=m/(ne^2\tau_{\rm ph}) \ , \tag{3}$$

where m is the mass of the free carries in concentration n and the lifetime $\tau_{\rm ph}$ is given by[8]

$$\frac{1}{\tau_{\rm ph}}=Ak_F\left[\frac{T}{\Theta}\right]^5\int_0^{\Theta/T}\frac{y^4}{e^y-1}dy \ . \tag{4}$$

Θ is the Debye temperature. The coefficient A is independent of T, and depends on the electron system only through a differential cross section σ_a. The variation of $\tau_{\rm ph}$ with x then mainly comes from the k_F factor in Eq. (3), so that $\tau_{\rm ph}^{-1}\propto k_F\propto n^{1/3}$, or, according to Eq. (4), $\rho_{\rm ph}\propto n^{-2/3}$. In the metallic configuration where $n\propto x$, we thus find $\rho_{\rm ph}\propto x^{-2/3}$; hence the decrease in the efficiency of the electron-phonon scattering mentioned in the preceding section, as x decreases.

ρ_m takes its origin in the Heisenberg exchange interaction H_m between the spin $\frac{1}{2}$ of the free carriers and the spin S of the localized spins. Its expression in function of the spin correlation function Γ^{AF} is well known.[8–13] In particular, near the magnetic ordering temperature,[10]

$$\begin{aligned}\rho_m(t)&=\rho_<+C|t|^{1/2}, \quad T<T_- \\ \rho_m(t)&=\rho_>-C|t|^{1/2}, \quad T>T_+\end{aligned} \tag{5}$$

where C is a constant. sgn(T) refers to the sign of the reduced temperature $t=(T-T_N)/T_N$. The temperatures $T_+(T_-)$ are larger (smaller), but close to T_N, and define the scaling regime (T_+, T_-) where the Landau theory breaks down.[14] Inside the scaling regime, the classical exponent $\frac{1}{2}$ has to be replaced by the exponent $1-\alpha$, with α the specific-heat exponent.[10] The onset of the antiferromagnetism is characterized by the increase of $\Gamma^{AF}(q,T)$ for $q\approx Q$, where Q is the wave vector associated with the magnetic structure. Moreover,

$$\frac{1}{N}\sum_{\mathbf{q}}\Gamma^{AF}(\mathbf{q},T)=\sum_{\mathbf{R}}\left[\frac{1}{N}\sum_{\mathbf{q}}e^{i\mathbf{q}\cdot\mathbf{R}}\right]\Gamma(\mathbf{R},T)$$
$$=\Gamma(R=0,T)=1\ , \tag{6}$$

since the expression in parentheses is just the delta distribution. Therefore, this sum rule, well known in nondiluted systems, remains valid when the distribution of magnetic ions is diluted. It follows from Eq. (6) that the sum over the magnetic fluctuations remains finite, i.e., the increase of $\Gamma^{AF}(q,T)$ for $q\approx Q$ upon cooling is at the expense of $\Gamma^{AF}(q,T)$ away from Q. Moreover, the wave vector of the momentum transfer q is such that $q<2k_F$, since the scattering of the free carriers by spin fluctuations is elastic. Therefore, ρ_m will increase upon cooling if Q is located inside the volume $Q<2k_F$, and will decrease in the opposite case. In Eq. (8), it means

$$C>0 \text{ if } Q<2k_F;\quad C<0 \text{ if } Q>2k_F\ . \tag{7}$$

Note that Eq. (6) is valid only when T is not too far from T_N, i,e., is in the critical regime. In particular, ρ_m becomes independent of T in the limit $T\gg T_N$ where $\Gamma^{AF}(R,T)\approx 0$ for $R\neq 0$. As a consequence, ρ in Eq. (1) reduces to $\rho_{\rm ph}$ except for a constant at temperatures $T>T_m$ with T_m the order of the temperature where ρ is minimum (70 K for the $x=0.7$ sample, for example). We took advantage of this property and determined the parameters A and Θ entering Eq. (4) from the fit of the $\rho(T)$ curves in the range $T>T_m$. Then, $\rho_{\rm ph}$ can be computed at all temperatures (including $T<T_m$). Finally, ρ_m is estimated by subtracting the theoretical $\rho_{\rm ph}(T)$ curve from the experimental $\rho(T)$ curve. The result is illustrated for $x=0.7$ in Fig. 7, where we have reported $\rho_m(T)-\rho_m(T\gg T_N)$ as a function of $\sqrt{T_N}\,\mathrm{sgn}(t)|t|^{1/2}$

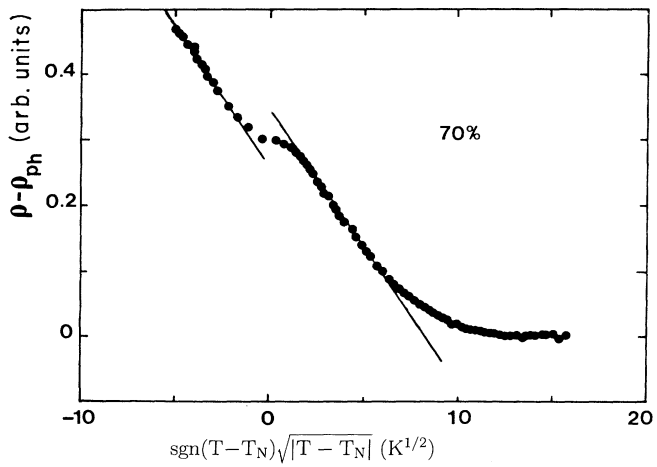

FIG. 7. Temperature dependence of the resistivity in $Yb_{1-x}Gd_xTe$ for $x=70\%$ in the vicinity of the Néel temperature T_N. The quantity reported on the abscissa has been chosen so that the plot should be linear (except close to T_N), after Eq. (11) in the text. The straight lines, with the same slope [C in the notations of Eq. (11)], drawn in the figure, can then be viewed as a theoretical fit of the resistivity curve, in the critical regime where the electron scattering by spin fluctuations dominates.

which, after Eq. (6), is the pertinent variable outside the scaling regime. Equation (6) is indeed well obeyed, with $T_{+,-}=T_N\pm 1$, $T_N=44$ K. The reduced temperature $|T_{+,-}-T_N|/T_N=2\%$ has the expected order of magnitude for the extension of the scaling region in magnetic materials.[15] The linear variation of $\rho_m(T)$ versus $\mathrm{sgn}(t)|t|^{1/2}$ is observed in the whole critical region $|T-T_N|<25$ K (except in the region $|T-T_N|<1$ K). For $T-T_N>25$ K, the variation of ρ_m as a function of T is getting smaller, and ρ_m becomes independent of T above 150 K for reasons we have already mentioned. In the range $|T-T_N|<1$ K, our data are not accurate enough, so that a quantitative analysis of $\rho_m(T)$ cannot be achieved. However, it is remarkable that the slope of the curve ρ versus $\mathrm{sgn}(t)|t|^{1/2}$ vanishes at $|t|=0$. Assuming that conventional scaling applies, it means that $\alpha<\frac{1}{2}$. However, an alternative and more likely interpretation is that the inhomogeneous distribution of magnetic ions, inherent in dilution, causes a smearing of the critical temperature, spreading in the range $T_-<T<T_+$. In this latter case, the specific heat will show a broadened peak of width $T_+-T_-=2$ K and a finite maximum at an average Néel temperature, instead of a divergence at a well defined T_N. Such behavior is mimicked by an exponent $\alpha<0$ that expresses that the inhomogeneities mask the true critical behavior. Therefore, specific-heat measurements are needed before any conclusion can be drawn in the range $|T-T_N|<1$ K.

B. Case $0.28\leq x\leq 0.5$

For such gadolinium concentrations, the previous equations fail to account for the experimental data, due to pretransitional effects, as one approaches the weak localization regime. Similar effects are observed in nonmagnetic semiconductors for a donor concentration close to the critical concentration x_m, where the metal-semiconductor transition takes place. However, a good estimate in nonmagnetic materials is given by the Mott criterion[16]

$$n^{1/3}a_B\approx 0.25\ , \tag{8}$$

with a_B the effective Bohr radius. In a standard material, the reduced dielectric constant and effective mass are typically $\varepsilon\approx 10$, $m\approx 0.1$, so x_m is of the order of 1%. In $Yb_{1-x}Gd_xTe$, we observe pretransitional effects at concentrations $x\leq 0.5$ at least one order of magnitude larger than expected from the Mott criterion. This feature is characteristic of magnetic materials. It is easily understood, if one approaches the MIT from the insulating side. Let us now consider the case of a magnetic semiconductor in its full generality, i.e., a material with magnetic ions and donors, which are not necessarily the same. Later, we will see the additional features associated with the specific case of $Yb_{1-x}Gd_xTe$, where the donors are also the magnetic ions. It is known that magnetic polaron effects lead to increased localization, with a donor electron orbital of size $r_0\approx d$, where d is the average distance between magnetic ions.[17] The electron associated with the bound magnetic polaron (BMP) will delo-

calize if the donor concentration reaches a value such that the BMP's orbitals on adjacent donors overlap. This will happen typically if the criterion in Eq. (8) is satisfied, with a_B now replaced by r_0:

$$n^{1/3}r_0 \approx 0.25 \ . \tag{9}$$

Since this condition is more stringent than Eq. (9), the BMP effect leads to an increase in the critical donor concentration at which the MIT takes place in magnetic semiconductors. There is another property specific to the case of interest here, where the magnetic ions are also the donor ions: a simple scaling argument $r_0 \approx d \approx x^{1/3}$, while $n \alpha x^{1/3}$ implies that $r_0 n^{1/3}$ does not depend on x, and is close to 0.25. It follows that the pretransitional regime on the metallic side of the MIT can extend over a broad range of Gd concentration, namely, $0.28 \leq x \leq 0.5$, according to experiments. This is also another drastic difference with the nonmagnetic materials where this regime can only be observed in a very narrow range of donor concentrations, because a_B is nearly independent of x in Eq. (9).

We now write

$$\rho = \rho_0' + \rho_{\rm ph} + \rho_{ml} \ , \tag{10}$$

where $\rho_{\rm ph}$ has the same meaning as in Eq. (1), ρ_{ml} is the contribution arising from Coulomb interactions, magnetic interactions, and localization effects in the random system. ρ_0' is the residual contribution to the resistivity issuing from other sources of electron scattering. The previous discussion shows that the localization regime is greatly influenced by the magnetic interactions in the material. The first consequence is that the Matthiessen rule cannot apply to ρ_{ml}, i.e., ρ_{ml} does not reduce to the sum of separate contributions from spin fluctuations, Coulomb and localization effects. According to the theory of random metals, the general form of the conduction is[18]

$$\rho_{ml}^{-1} = \sigma_0 + mT^{\beta} + BT \ . \tag{11}$$

σ_0 is the zero-temperature contribution of the scattering mechanisms involved in ρ_{ml}^{-1}. Coulomb interactions with electron-electron scattering in the presence of random impurities (Gd^{3+} in the occurrence) give $\beta = \frac{1}{2}$ and a magnitude m that can change sign as the size of the screening length varies.[19–22] Such behavior has been observed in nonmagnetic materials, for example in Si:P, with m changing sign as n varies, while $\beta = \frac{1}{2}$ close to the metal-insulator transition,[23] or in Ge:Sb.[24,25] More recently, a similar $T^{1/2}$ behavior has also been reported in magnetic[26] and semimagnetic[27] semiconductors. The linear BT term in Eq. (11) arises from localization theory.[28] In three-dimensional systems, the diffusion coefficient $D(\omega)$ of a particle with energy E in the presence of a random field is[28]

$$D(\omega) = D_0 \left[1 + \frac{3\hbar^2 \sqrt{6\omega\tau}}{16E^2\tau^2} \right] \ , \tag{12}$$

with ω the frequency and τ the relaxation time of the particle. Thus, the quantum correction is proportional to $\omega^{1/2}$. In addition, the energy relaxation process will act as a cutoff at $\omega = 1/\tau_E$. Therefore, the correction to the conductivity is

$$\Delta\sigma \alpha (1/\tau_E)^{1/2} \ . \tag{13}$$

If the energy relaxation lifetime τ_E is due to the electron-electron scattering, one has[29] $(1/\tau_E) \alpha T^2$; hence the linear term $\Delta\sigma = BT$ in Eq. (11).

In any disordered system, the $T^{1/2}$ behavior of the conductivity due to the second term in Eq. (11) could be observed only at very low temperatures ($T < 1$ K). All our experiments have been made in the opposite range $T > 1$ K, where the $T^{1/2}$ term is expected to be negligible with respect to the T term, so that Eq. (11) reduces to

$$\rho_{ml}^{-1} \approx \sigma_0 + BT \ . \tag{14}$$

We have already noticed that the relative contribution of $\rho_{\rm ph}$ to ρ is getting smaller as x decreases, partly because $1/\tau_{\rm ph}$ decreases as $n(E_F)$ (hence x) decreases according to Eq. (4), and also because ρ_{ml} is increasingly important. The best sample to use to probe Eq. (14) is thus the sample with the lowest Gd concentration ($x = 0.28$) for which $\rho \approx \rho_{ml}$ in a range of temperatures that extends to 60 K. The plot of ρ^{-1} as a function of T in this range is illustrated in Fig. 8, which shows that Eq. (14) is quantitatively satisfied. Data up to room temperature can be fitted by Eq. (11), with $\rho_{\rm ph}$ still given by Eqs. (3) and (4), in which A is the only fitting parameter, while Θ is kept equal to its value $\Theta = 500$ K deduced from the analysis of $\rho(T)$ for $x = 0.7$. At first sight, it seems that a fit of $\rho(T)$ in the whole temperature range $10 < T < 300$ K depends on four parameters (ρ, σ_0, A, and B). However, above 10 K, the temperature is high enough so that σ_0 is much smaller than BT in Eq. (14) (see Fig. 8). Therefore, a good approximation consists in writing Eq. (11) in the form

$$\rho = \gamma + \delta/T + \rho_{\rm ph} \ , \tag{15}$$

so that the number of fitting parameters is actually re-

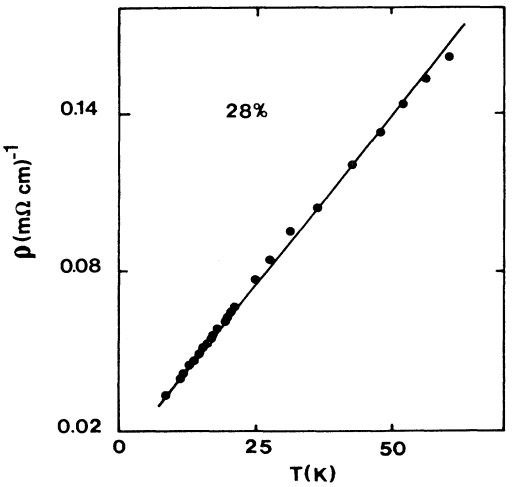

FIG. 8. Temperature dependence of the conductivity of $Yb_{1-x}Gd_xTe$ for $x = 0.28$. The straight line is theoretical.

duced to three (γ, δ, and A). In addition, ρ_{ph} has nonnegligible effects only at high temperature, so that γ and δ are determined unambiguously from the fit of $\rho(T)$ at low temperature (say, $T < 100$ K), while A is determined from the fit of the $\rho(T)$ curve at high temperature. Therefore, the fit of $\rho(T)$ curves by Eqs. (10) and (14) is unique. Moreover, ρ_{ph} is only a small correction to the resistivity for $x < 0.5$ (see Fig. 6). Similar fits of the resistivity curves are illustrated for two other concentrations, $x = 0.35$ and $x = 0.5$, in Fig. 5. The fits of the $\rho(T)$ curves for $x = 0.35$ and $x = 0.28$ are equally good. By contrast, the $\rho(T)$ curve for $x = 0.5$ is fitted by our model only for $T > T_N$. We have already noticed that Matthiessen's rule cannot apply for $x = 0.5$, so the effect of antiferromagnetic ordering on resistivity cannot be described quantitatively by Eqs. (5) and (7). Nevertheless, we can still refer to them for a qualitative analysis to explain why $\rho(T)$ is below the theoretical value at $T < T_N$: at $x = 0.5$, the carrier concentration is small enough so that the condition $Q > 2k_F$ is fulfilled in Eq. (7); hence, $C < 0$ and antiferromagnetic ordering reduces the diffusion of the free carriers by the localized spin system.

On the other hand, the fact that Eqs. (10) and (11) fit the $\rho(T)$ curve down to the lowest temperature investigated, for $x = 0.35$ and 0.28, is evidence that no antiferromagnetism takes place for such gadolinium concentrations, in agreement with our previous statement that the magnetic percolation threshold for long-range magnetic ordering is $x_c \cong 0.4$.

C. Case $x \leq 0.2$

In Sec. III C, we used a scaling argument to infer that $r_0 n^{-1/3}$ is independent of x. If it were true, the criterion in Eq. (9) would never be fulfilled and the material would remain metallic at any x. This, however, is not true, because the scaling argument misses an ingredient: the electron wave function in a BMP must be normalized. Therefore, as x decreases, the increase of r_0 is at the expense of electron density at the magnetic sites inside the BMP. Since the magnetic exchange energy is proportional to this electron density, the magnetic binding energy will decrease accordingly; hence an additional increase of the orbital radius r_0 with respect to the simple relation $r_0 \alpha x^{-1/3}$. Therefore, $r_0 n^{-1/3}$ decreases as x decreases and the criterion in Eq. (1) is reached at a finite concentration $x = x_m$. For $x \leq 0.2$, the resistivity curves cannot be described by Eqs. (10), (11), or (15). Instead, an activated regime is observed in the paramagnetic configuration ($T > 17$ K):

$$\rho \alpha e^{E_A/kT}, \tag{16}$$

which shows that we are now on the semiconductor side of the MIT. This is evidenced in Fig. 9. Therefore, $x_m = 0.24 \pm 0.03$, one order of magnitude larger than predicted by the Mott criterion in Eq. (14), for reasons we have already discussed. Note that the activation energy is small ($E_A = 65$ K for $x = 0.2$), which suggests that the conductivity at finite temperature arises from a hopping mechanism due to thermal activation above a mobility edge.[30] Deviations from this activation regime are observed for $T \leq T_f$, with T_f the spin-freezing temperature, equal to ≈ 17 K for this $x = 0.2$ sample (see Fig. 2). This is because the local freezing of spin fluctuations modifies the landscape of the disordered potential experienced by the electrons via indirect exchange mechanism. As a result, $\rho(T)$ at $T < T_f$ is still of the activated form [Eq. (16)] with, however, a reduced activation energy $E_A/k_B = 40$ K as compared with 65 K at $T > T_f$ for $x = 0.2$.

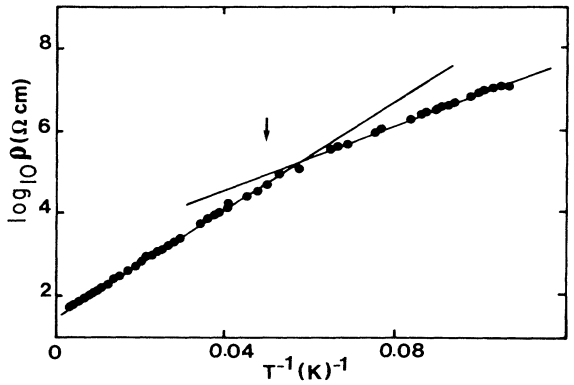

FIG. 9. Resistivity curve of the $x = 20\%$ sample versus the inversion of the temperature, which illustrates the activated regime. Note the change of slope (i.e., the change in the activation energy) on both sides of the freezing temperature T_f, marked by an arrow.

IV. DISCUSSION

The magnetic (or semimagnetic) semiconductors form a family that includes a great number of materials already extensively studied. It is then desirable to discuss the physical properties of the new solid solution $Yb_{1-x}Gd_xTe$ with respect to other members of this family.

The europium chalcogenides are the best known examples of chalcogenides where, as in $Yb_{1-x}Gd_xTe$, divalent rare-earth ions can be substituted by Gd^{3+} ions acting as donors. A comprehensive review of their physical properties can be found in Ref. 4. However, Yb^{2+} is nonmagnetic, in contrast with Eu^{2+}, which caries the spin $S = \frac{7}{2}$, like Gd^{3+}. As a consequence, both magnetic and transport properties are markedly different in those two cases. For instance, the paramagnetic Curie temperature Θ_p is a monotonic decreasing function of x (in algebraic value)[1] in the whole range $0.4 < x < 1$ where the solid solution orders antiferromagnetically. On the other hand, Θ_p oscillates with x in $Eu_{1-x}Gd_xS$ and $Eu_{1-x}Gd_xO$ due to the oscillations of the RKKY exchange parameter as a function of $k_F R$ in Eq. (1).[31] This difference comes from the fact that $k_F R$ is independent of x, since $k_F \alpha x^{1/3}$ and $R \alpha x^{-1/3}$ in metallic $Yb_{1-x}Gd_xTe$ while $k_F R \alpha x^{1/3}$ in $Eu_{1-x}Gd_xS$ and $Eu_{1-x}Gd_xO$ solutions, where the mean distance between the magnetic ions remains constant.

Another kind of semimagnetic semiconductors is generated by II-VI and IV-VI compounds, in which cations have been substituted by magnetic ions, usually Mn^{2+}.

Thanks to the fact that these materials are archetypes of Heisenberg spin glasses, they also have been extensively studied in the past. In particular, their magnetic percolation threshold x_c for the onset of long-range magnetic ordering is well known, allowing for a direct comparison with $x_c \approx 0.4$ we found in $Yb_{1-x}Gd_xTe$. This is a typical order of magnitude observed in materials where the antiferromagnetic interactions are short range. For example, $x_c \approx 0.7$ in $Cd_{1-x}Mn_xTe$, which also crystallizes in the fcc lattice with antiferromagnetic interactions mainly restricted to nearest neighbors.[32] In $Yb_{1-x}Gd_xTe$, however, the excess conduction electrons supplied by the Gd^{3+} ions mediate a RKKY interaction. In the free-electron approximation, this RKKY interaction decays very slowly (in R^{-3}). The large value of x_c observed in $Yb_{1-x}Gd_xTe$ suggests that the mean free path of the conduction electrons plays the role of a cutoff for the indirect interaction and must be comparable to the lattice parameter. This is actually confirmed by the transport measurements, which show that the electron mobility $\mu = 1/(ne\rho) \approx 1$ cm^2/V s for $x = 0.5$ and $T = 10$ K. Such a small mobility is indeed characteristic of a mean free path λ the order of few Å. In the absence of magnetic interactions, λ should be much larger, since the Mott criterion predicts that localization effects should be negligible for $x > 1\%$. The magnetic interaction of the conduction electrons with its Gd^{3+} neighbors then plays a key role in the localization, through the so-called magnetic polaron effect. Localization thus occurs because of the combined effect of the random potential fluctuations and magnetic polaron effects. Note that the polaron effect only applies to an antiferromagnetic lattice at low temperatures, since no spin polarization, hence no magnetic energy, can be gained in a localization process if all the spins of the magnetic sites are already saturated ferromagnetically in the delocalized state. This argument explains the difference between $x_c = 0.4$ for the antiferromagnetic percolation threshold met in this work, and $x_c = 0.03$ for the ferromagnetic percolation threshold in $Sn_{1-x}Mn_xTe$.[33]

Transport measurements reveal that the metal-insulator transition takes place at a Gd concentration $x_m \approx 0.2$. The electrons are more sensitive to local magnetic clustering if they are in a localized state, hence the change in activation energy of the resistivity curve in the vicinity of the spin-freezing temperature, for $x < x_m$. On another end, for $x \geq 0.28$, the electrons are delocalized, and thus sensitive to the onset of long-range magnetic correlations. Hence, a change in the resistivity curve upon antiferromagnetic ordering, for $x > x_c$. In the intermediate range $x_m < x < x_c$, the diffusion of the electrons by spin fluctuations does not contribute significantly to the temperature dependence of the resistivity. This range of composition is thus best suited to probing the theories of disordered metals.

A lot of experimental works in nonmagnetic materials have been devoted to this subject in the past. Nevertheless, they could give only incomplete information regarding the diffusion of interacting electrons into the region of strong scattering near the critical point of the MIT. While the $T^{1/2}$ behavior of the conductivity for $T \ll 1$ K is commonly observed, the only work, to our knowledge, that gives experimental support to the existence of an additional linear BT term in Eq. (11) is that of Thomas *et al.*[24] These authors have shown that the deviation from the $T^{1/2}$ behavior of the conductivity above 150 mK in Ge:Sb can be attributed to the BT term. However, other corrections may fit the data as well, according to the authors themselves. In particular, disorder effects lead to $1/\tau_E \alpha T^{3/2}$,[34] which, according to Eq. (14), leads to a conductivity term in $T^{3/4}$. The range of temperatures explored in Ref. 18, $150 < T < 500$ mK, is too short to distinguish between a $T^{3/4}$ and T behavior, inasmuch as such terms are small with respect to the $mT^{1/2}$ term at such low temperatures. Instead of measuring $\sigma(T)$ for fixed carrier concentrations, it is also possible to investigate $\sigma(T=0)$ as a function of n. Scaling arguments lead to[35,36]

$$\sigma(T=0) \approx (E_F - E_c)^{\nu} , \tag{17}$$

which may also be written[37]

$$\sigma(T=0) = \sigma_{\min}(n/n_c - 1)^{\nu} , \tag{18}$$

with E_F the Fermi energy and E_c the mobility edge. n_c is the critical concentration at the MIT. In principle, the exponent should tell something about the nature of the diffusion mechanism at the MIT. However, in nonmagnetic materials, there is no unique experimental value of ν, which ranges from 0.5 (Ref. 37) to 1.[38,39]

The exponent ν has also been explored in magnetic semiconductors $Gd_{3-x}v_xS_4$,[26] $Cd_{1-x}Mn_xSe$, and $Hg_{1-x}Mn_xTe$.[27] While Eq. (18) is a scaling law at zero magnetic field as a function of n, the exponent ν in magnetic semiconductors has been developed from the similar scaling law at fixed n (i.e., for a given sample) as a function of the applied magnetic field H:

$$\sigma(T=0,H) \approx (H - H_c)^{\nu} , \tag{19}$$

resulting from the linear dependence of $E_F - E_c$ with H.[26] According to Eq. (19), a metal-insulator transition is driven by the magnetic field, at the critical value H_c. In the case ν is deduced from the measurements of the conductivity at magnetic fields $H \geq H_c$, such that the magnetic length $L_H = (h/eH)^{1/2}$ is not negligible with respect to the phase-breaking length $L_\phi = (hD/k_BT)^{1/2}$ with D the diffusion coefficient.[27] Under such circumstances, the theories of the MIT in a system of noninteracting electrons in a random potential predict $\nu = \frac{1}{2}$,[40] compared with the experimental value $\nu = 1$.[26,27] On the other hand, the theory that takes the Coulomb interactions among electrons into account in the case of carriers in one spin-up subband predicts $\nu = 1$ for all the semimagnetic semiconductors investigated in Refs. 26 and 27 which is then further evidence of the dominant role played by Coulomb interactions in such materials.

V. CONCLUSION

In conclusion, we have presented evidence of outstanding T^{-1} behavior of the zero-field resistivity, which we attribute to the quantum corrections to the electron

scattering mechanism in the critical regime of the metal-insulator transition. This feature is consistent with the value of the exponent $\nu=1$ found in semimagnetic semiconductors for the magnetic-field dependence of magnetoresistivity at high fields. These results show that the Coulomb electron-electron interaction is enhanced by magnetic fluctuations via the exchange interaction, and plays the key role in the strong diffusion regime. In particular, electron-interaction effects overcome the weak localization contribution[34,35,41] which is not caused by this interaction. In the insulating side, close to the MIT, an activated regime of the resistivity curve is observed, with a small activation energy typical of a thermal activation of the electrons of bound magnetic polarons above a mobility edge. This can be understood, if we note that the magnetically enhanced electron interaction effects are also dominant, in this regime where metallic screening is absent.

ACKNOWLEDGMENTS

Groupe de Physique des Solides is Unité de Recherche Associé No. 17 du CNRS.

[1]R. Davot and A. Mauger, J. Alloys Compounds **178**, 229 (1992).

[2]J. R. McGuire, R. J. Gambino, S. J. Pickart, and H. A. Alperin, J. Appl. Phys. **40**, 1009 (1969).

[3]For reviews, see *Localization, Interaction and Transport Phenomena,* edited by B. Kramer *et al.* (Springer, Berlin, 1985); R. A. Lee and T. V. Ramakrishnan, Rev. Mod. Phys. **57**, 287 (1985).

[4]For a review, see A. Mauger and C. Godart, Phys. Rep. **141**, 51 (1986).

[5]M. A. Ruderman and C. Kittel, Phys. Rev. **96**, 99 (1954); T. Kasuya, Prog. Theor. Phys. **16**, 45 (1966); K. Yosida, Phys. Rev. **106**, 893 (1957).

[6]P. G. de Gennes, J. Phys. Radium **23**, 630 (1962).

[7]B. L. Altshuler, A. G. Aronov, and A. Yu. Zuzin, Zh. Eksp. Teor. Fiz. **84**, 1525 (1983) [Sov. Phys. JETP **57**, 889 (1983)]; Pis'ma Zh. Eksp. Teor. Fiz. **38**, 128 (1983) [JETP Lett. **38**, 153 (1979)]; A. M. Finkelstein, Pis'ma Zh. Eksp. Teor. Fiz. **40**, 63 (1984) [JETP Lett. **40**, 796 (1984)]; C. Castellani, C. Di Castro, P. A. Lee, M. Ma, S. Sorella, and E. Tabet, Phys. Rev. B **30**, 1596 (1984).

[8]See, for example, J. M. Ziman, *Principles of the Theory of Solids* (Cambridge University Press, 1964), p. 189.

[9]P. G. de Gennes and J. Friedel, J. Phys. Chem. Solids **4**, 71 (1958).

[10]M. E. Fisher and J. S. Langer, Phys. Rev. Lett. **20**, 665 (1968).

[11]T. G. Richard and D. J. W. Geldart, Phys. Rev. Lett. **30**, 665 (1968).

[12]D. J. W. Geldart and T. G. Richard, Phys. Rev. B **12**, 5175 (1975).

[13]T. G. Richard and D. J. W. Geldart, Phys. Rev. B **15**, 303 (1977).

[14]H. B. Tarko and M. E. Fisher, Phys. Rev. B **11**, 1217 (1975).

[15]I. Balberg, Physica **91B**, 71 (1977).

[16]N. F. Mott, *Metal-Insulator Transitions* (Taylor and Francis, London, 1974); N. F. Mott and E. A. Davis, *Electronic Processes in Non-Crystalline Materials* (Oxford University Press, Oxford, 1979).

[17]A. Mauger and D. L. Mills, Phys. Rev. Lett. **53**, 1594 (1984); Phys. Rev. B **31**, 8024 (1985).

[18]G. A. Thomas and A. Kawakaba, Phys. Rev. B **26**, 2133 (1982).

[19]B. L. Altshuler and A. G. Aronov, Zh. Eksp. Teor. Fiz. **77**, 2028 (1979) [Sov. Phys. JETP **50**, 968 (1979)]; Pis'ma Zh. Eksp. Teor. Fiz. **27**, 700 (1978) [JETP Lett. **27**, 662 (1978)]; **30**, 514 (1979) [**30**, 482 (1979)].

[20]B. L. Altshuler and A. G. Aronov, Solid State Commun. **36**, 115 (1979).

[21]B. L. Altshuler, A. G. Aronov, and P. A. Lee, Phys. Rev. Lett. **44**, 1288 (1980); B. L. Altshuler, D. Kmel'nitzkii, A. I. Larkin, and P. A. Lee, Phys. Rev. B **22**, 5142 (1980); B. L. Altshuler and A. G. Aronov, Solid State Commun. **38**, 11 (1981).

[22]P. A. Lee and T. V. Ramakrishnan, Phys. Rev. B **26**, 4009 (1982).

[23]T. F. Rosenbaum, K. Andres, G. A. Thomas, and P. A. Lee, Phys. Rev. Lett. **46**, 568 (1981).

[24]G. A. Thomas, A. Kawabata, Y. Ootuka, S. Katsumoto, S. Kobayashi, and W. Sasaki, Phys. Rev. B **24**, 4886 (1981); C. Yamanouchi, K. Mizuguchi, and W. Sazuki, J. Phys. Soc. Jpn. **22**, 859 (1967).

[25]G. A. Thomas, A. Kawabata, Y. Ootuka, S. Katsumoto, S. Kobayashi, and W. Sasaki, Phys. Rev. B **26**, 2113 (1982).

[26]S. Von Molnar, A. Briggs, J. Flouquet, and G. Remengi, Phys. Rev. Lett. **51**, 706 (1983).

[27]T. Wojtowicz, T. Dietl, M. Sawicki, W. Plesiewicz, and J. Jaroszynski, Phys. Rev. Lett. **56**, 2419 (1986).

[28]L. P. Gor'kov, A. I. Larkin, and D. E. Khmel'nitzkii, Pis'ma Zh. Eksp. Teor. Fiz. **30**, 248 (1979) [JETP Lett. **30**, 228 (1979)].

[29]J. J. Quinn and R. A. Fersell, Phys. Rev. **112**, 812 (1958).

[30]M. H. Cohen, E. N. Economou, and C. M. Soukoulis, Phys. Rev. Lett. **51**, 1202 (1983).

[31]A. Mauger, Phys. Status Solidi B **84**, 761 (1977).

[32]For reviews, see, e.g., *Diluted Magnetic Semiconductors,* edited by J. K. Furdyna and J. Kossut, Semiconductors and Semimetals Vol. 25 (Academic, Boston, 1988); J. K. Furdyna, J. Appl. Phys. **64**, R29 (1988).

[33]A. Mauger and M. Escorne, Phys. Rev. B **35**, 1902 (1987).

[34]A. Schmidt, Z. Phys. **271**, 251 (1974); E. Abrahams, P. W. Anderson, P. A. Lee, and T. V. Ramakrishnan, Phys. Rev. B **24**, 6783 (1982).

[35]E. Abrahams, P. W. Anderson, D. C. Licciardello, and T. V. Ramakrishnan, Phys. Rev. Lett. **42**, 673 (1979).

[36]Y. Imry, Phys. Rev. Lett. **44**, 469 (1980).

[37]T. F. Rosenbaum, K. Andres, G. A. Thomas, and R. N. Bhatt, Phys. Rev. Lett. **45**, 1723 (1980).

[38]R. C. Dynes and J. P. Garno, Phys. Rev. Lett. **46**, 137 (1981).

[39]G. Hertel, D. J. Bishop, E. G. Spencer, J. M. Rowell, and R. C. Dynes, Phys. Rev. Lett. **50**, 743 (1983).

[40]K. B. Efetov, Adv. Phys. **32**, 53 (1983), and references therein; A. Kawabata, Solid-State Electron. **28**, 131 (1985).

[41]P. W. Anderson, E. Abrahams, and T. V. Ramakrishnan, Phys. Rev. Lett. **43**, 718 (1979).